1

Observer-based Sliding Mode Load Frequency Control of Power Systems Under Deception Attack

1.1 Background

Developments in power systems have greatly improved human life. Ensuring stability and sustainability of power systems, as an increasingly important research area, has attracted extensive attention [1–3].

One of the most popular goals of such studies is to ensure stable operation of the power system, to which the use of control methods helps provide a boost [4, 5]. Sliding mode control (SMC), with its advantages in overcoming system uncertainties and achieving strong robustness against disturbances, has been widely used in a variety of fields [6–8]. System robustness is enhanced by combining dynamic surface control with sliding mode [9–12]. It can be used in different systems like nonlinear systems [13], Markovian jump systems [14], power systems, and so on. Here, we focus on the power system. The robust stability of adaptive event-triggered load frequency control (LFC) with SMC for multi-area power systems is investigated in [4]. The authors Huang and Wang [15] proposed a fractional-order sliding mode controller for effectively stabilizing a nonlinear power system in a fixed time. In [16], a highly robust observer sliding mode-based load frequency and tie-power control to compensate for primary frequency control of multi-area interconnected power systems was designed. While the power system can be kept stable by SMC, the modern power system relies on the critical cyber infrastructure, which makes it vulnerable to hostile cyber threats.

Some robust control methods are applied to the LFC of the multi-area power system. It should be pointed out that in the analysis of multi-area power system problems, the attacks from outside the system may be ignored. There are many types of cyberattacks that can act on the power systems, among them include denial-of-service attack, deception attack, and data integrity attack, etc [17–21]. A deception attack is to compromise the trustworthiness of data by manipulating the packets transmitted over the communication networks. When under a deception attack, the flow of information in the system will be changed [22, 23], which may destabilize or even crash the system.

We pay special attention to the deception attack in this chapter. In [24], a new malicious data deception attack by considering a practical attacking situation was investigated. An active synchronous detection method was proposed in [25] to detect deception attack in microgrids without impeding system operations. In [26], the authors investigated the viability of machine learning methods in detecting cyberattacks. Considering the impact of damaged information, the observer-dependent event-triggered scheme is applied in this chapter. The event-trigger control works only when a certain set of event-trigger conditions are met. Using this method can not only make effective use of communication resources, but also prolong the service time of the controller. This makes it be rapidly developed in the system control, especially in dealing with complex networked dynamic systems. A properly designed event-triggering scheme may also help us find out whether the system is under malicious attack. In [27], a dynamic event-triggered mechanism was proposed to modulate the transmission of data packets. The cooperative control problem has been investigated based on a novel event-triggered scheme in [28]. The random deception attack is well handled according to a memory-based event-triggered scheme proposed in [29]. In [30], a mathematical model concerning the event-triggered LFC under deception attack was developed. The collaborative design of both the event-trigger strategy and the adaptive robust controller is investigated in [31]. The authors in [32] investigated the observer-based predictive event-triggered LFC for a smart grid incorporating electric vehicles. Benefiting from the use of an event-triggered mechanism, the negative impacts of deception attack on information transmission can be effectively detected. Based on which the control module may work in time to ensure the stable operation of the system.

We design an observer-based sliding mode LFC scheme for controlling multi-area power systems under deception attack. Firstly, by taking into account the characteristic of the deception attack, a model of attacked power system is built. Then, an observer is proposed to estimate the state of the damaged system. Further, the event trigger is introduced to judge whether the normal operation of the system is compromised using the designed event trigger conditions. The main contributions of this chapter can be generalized as follows:

1. A novel SMC is proposed for the multi-area power systems under deception attack. The proposed observer-based event-trigger SMC helps save the limited network channel resources, so that the desired control can be performed successfully.

2. The sliding mode load frequency problem in an interconnected power system with a deception attack is well-analyzed. Considering the designed SMC surface, the equivalent control under the basic SMC is obtained through analysis. The observer and the event triggering scheme are introduced to analyze the power system under deception attack. Using the linear matrix inequality (LMI) method, the conditions of the system's asymptotic stability are obtained. Finally, an appropriate SMC law is designed to ensure the reachability of the system trajectory.

1.2 Problem Formulation

1.2.1 Model Description

The multi-area power system is a type of complex control system. In this section, the control problem of a sliding mode LFC-based power system under deception attack is analyzed. The i-th area of a power system under deception attack model is shown in Figure 1.1, which consists of a generator, a governor and a turbine, and so on. The meanings of the notations in Figure 1.1 are shown in Table 1.1.

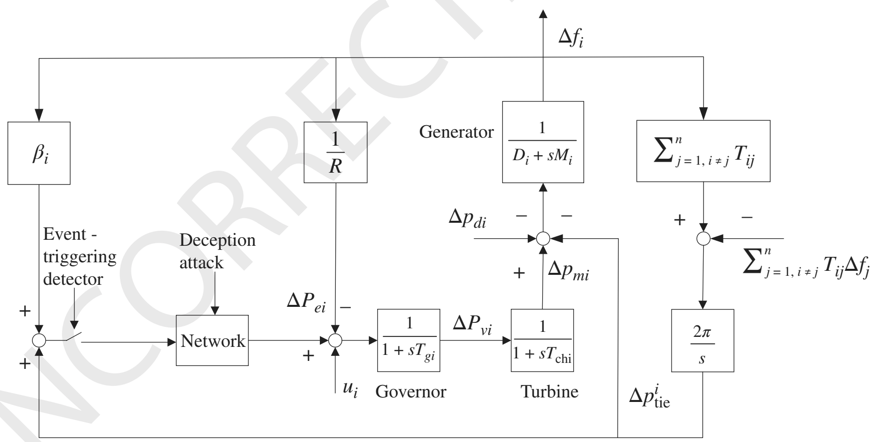

Figure 1.1 The model of the i-th area of the power system.

Table 1.1 Definition of notations.

Δf_i	Frequency deviation
ΔP_{tie}^i	Deviation of tie-line power exchange between areas
ΔP_{mi}	Mechanical output deviation
ΔP_{di}	Load deviation
D_i	Damping coefficient
M_i	Inertia of the generator
ΔP_{vi}	The deviation value
R_i	Droop coefficient
T_{gi},	Time constant of the governor
u_i	Control input
T_{chi}	Time constant of the turbine
T_{ij}	Synchronization coefficient between areas

Based on the system model and information transfer, the dynamic equation of the system can be obtained as follows

$$\begin{cases} \Delta \dot{P}_{mi}(t) = -\dfrac{\Delta P_{mi}(t)}{T_{\text{chi}}} + \dfrac{\Delta P_{vi}(t)}{T_{\text{chi}}} \\ \Delta \dot{P}_{ei}(t) = \Delta P^i_{\text{tie}}(t) + \beta_i \Delta f_i(t) \\ \Delta \dot{P}^i_{\text{tie}}(t) = -2\pi \displaystyle\sum_{j=1, i\neq j}^{n} T_{ij}(\Delta f_i(t) - \Delta f_j(t)) \\ \Delta \dot{P}_{vi}(t) = \dfrac{u_i(t)}{T_{gi}} - \dfrac{\Delta f_i(t)}{R_i T_{gi}} - \dfrac{\Delta P_{vi}(t)}{T_{gi}} - \dfrac{\Delta P_{ei}(t)}{T_{gi}} \\ \Delta \dot{f}_i(t) = \dfrac{\Delta P_{mi}(t)}{M_i} - \dfrac{\Delta P_{di}(t)}{M_i} - \dfrac{D_i \Delta f_i(t)}{M_i} - \dfrac{\Delta P^i_{\text{tie}}(t)}{M_i} \end{cases} . \tag{1.1}$$

We can derive the state equation of i-th area power system as

$$\begin{cases} \dot{x}(t) = Ax(t) + Bu(t) + Fw(t) \\ y(t) = Cx(t) \end{cases} \tag{1.2}$$

where $w(t)$ is the disturbance of the system and defined as $w(t) = \Delta P_{di}$, $w(t)$ is bounded and satisfies $\Delta P_{\text{di}} < h_i$, h_i is the positive constants,

$$x_i(t) = [x_1^T(t), x_2^T(t), \cdots, x_n^T(t)]^T,$$

$$u(t) = [u_1^T(t), u_2^T(t), \cdots, u_n^T(t)]^T,$$

$$y_i(t) = [y_1^T(t), y_2^T(t), \cdots, y_n^T(t)]^T,$$

$$w_i(t) = [\Delta P_{d1}(t), \Delta P_{d2}(t), \cdots, \Delta P_{dn}(t)]^T,$$

$$x(t) = [\Delta f_i, \Delta P_{mi}, \Delta P_{vi}, \Delta P_{ei}, \Delta P^i_{tie}]^T.$$

where A, B, C, and F are the parameter matrixes, $A = [A_{ij}]_{n\times n}$, $B = \text{diag}\{\underbrace{B_1, \cdots, B_i}_{n}\}$, $C = \text{diag}\{\underbrace{C_1, \cdots, C_i}_{n}\}$, $F = \text{diag}\{\underbrace{F_1, \cdots, F_i}_{n}\}$.

$$A = \begin{bmatrix} -\frac{D_i}{M_i} & \frac{1}{M_i} & 0 & 0 & -\frac{1}{M_i} \\ 0 & -\frac{1}{T_{\text{chi}}} & \frac{1}{T_{\text{chi}}} & 0 & 0 \\ -\frac{1}{R_i T_{gi}} & 0 & -\frac{1}{T_{gi}} & 0 & 0 \\ \beta_i & 0 & 0 & 0 & 1 \\ -2\pi \sum\limits_{j=1, j\neq i}^{n} T_{ij} & 0 & 0 & 0 & 0 \end{bmatrix},$$

$$B = \begin{bmatrix} 0 & 0 & \frac{1}{T_{\text{gi}}} & 0 & 0 \end{bmatrix}^T, F = \begin{bmatrix} 0 & 0 & 0 & 0 & -\frac{1}{M_i} \end{bmatrix}^T.$$

1.2.2 Event-triggered Control

The data information of the power system is transmitted by the shared network to the corresponding sliding mode controller. In this section, a sliding mode observer-based load frequency controller for the ith-area power systems is given. An event-triggered scheme will be put forward taking into account the consideration of the deception attack

$$\tilde{y}(t) = (1 - \alpha(t))y(t) + \alpha(t)\varepsilon(t), \tag{1.3}$$

where $\varepsilon(t)$ is the deception attack from outside of the system and $\alpha(t)$ is an energy-bounded signal belonging to $L_2 \in [0, +\infty)$. $\alpha(t)$ is a stochastic variable subject to a Bernoulli distribution satisfying

$$\begin{cases} P\{\alpha(t) = 1\} = \mathbb{E}\{\alpha(t)\} := \alpha_0 \\ P\{\alpha(t) = 0\} = 1 - \mathbb{E}\{\alpha(t)\} := 1 - \alpha_0 \end{cases} \tag{1.4}$$

When the deception attack happens, the information transmitted will be changed, the system equation of state can be expressed as

$$\begin{cases} \dot{x}(t) = Ax(t) + Bu(t) + Fw(t) \\ \widetilde{y}(t) = (1 - \alpha(t))Cx(t) + \alpha(t)\varepsilon(t) \end{cases} \tag{1.5}$$

Using the observed information as the transmitted information. To facilitate the analysis of the problem, the state of the observed information is defined as $\hat{x}(t)$, then

$$\begin{cases} \dot{\hat{x}}(t) = A\hat{x}(t) + Bu(t) + L(\tilde{y}(t) - \hat{y}(t)) \\ \hat{y}(t) = (1 - \alpha(t))C\hat{x}(t) \end{cases}. \tag{1.6}$$

To facilitate the detection of the deception attack on the system, the event-trigger is used in the system model 1.1. In the absence of deception attack, a common event-triggered condition [33] is given as

$$\begin{aligned} &t_{k+1}h = t_k h + \\ &\min_{d\in\mathbb{R}^+}\{dh \| e^T(j_k h)\phi e(j_k h) \geq \delta(t_k h)\hat{x}^T(t_k h)\phi\hat{x}(t_k h)\} \end{aligned}, \tag{1.7}$$

where $\phi = \eta C^T C, \eta$ is a positive definite matrix, and $\phi = \mathrm{diag}\{\phi_1, \cdots, \phi_n\}$ is defined as a weighting matrix. We denote the information error as $e(j_k h) = \hat{x}(j_k h) - \hat{x}(t_k h)$, $j_k h = t_k h + dh$, $d \in \mathbb{R}_0^+$. δ is a predefined scalar confined in the interval $[0, 1)$.

The system error is $\Theta(t) = x(t) - \hat{x}(t)$. Then

$$\begin{aligned} \dot{\Theta}(t) &= A\Theta(t) + Fw(t) \\ &\quad - L(\alpha(t)\varepsilon(t) + (1 - \alpha(t))C\Theta(t)) \end{aligned}. \tag{1.8}$$

1.2.3 Sliding Mode Design

To make the system working stable, the SMC method is introduced. We construct the following sliding mode surface function

$$\sigma(t) = G\hat{x}(t) - \int_0^t G(A + BK)\hat{x}(\tau)d\tau, \tag{1.9}$$

where G is a constant matrix and it is selected to ensure that GB stays nonsingular, $0 \leq \tau(t) \leq h + \tau_{\max}, \tau_{\max} > 0$.

We all know that the switch surface function should satisfy

$$\sigma(t) = 0 \text{ and } \dot{\sigma}(t) = 0. \tag{1.10}$$

The derivative of the sliding surface is

$$\dot{\sigma}(t) = G\dot{\hat{x}}(t) - GA\hat{x}(t) - GBK\hat{x}(t). \tag{1.11}$$

According to (1.6) and (1.11), we have

$$\begin{aligned}\dot{\sigma}(t) &= G[A\hat{x}(t) + Bu(t) + L(\tilde{y}(t) - \hat{y}(t))] \\ &\quad - GA\hat{x}(t) - GBK\hat{x}(t) \\ &= -GBK\hat{x}(t) + GBu(t) + GL(\tilde{y}(t) - \hat{y}(t))\end{aligned}. \tag{1.12}$$

Noticing the function (1.10), we have

$$-GBK\hat{x}(t) + GBu(t) + GL(\tilde{y}(t) - \hat{y}(t)) = 0. \tag{1.13}$$

Thus, we get the equivalent controller

$$u_{\mathrm{eq}} = K\hat{x}(t) - (GB)^{-1}GL(\tilde{y}(t) - \hat{y}(t)). \tag{1.14}$$

Then, the controlled system and the error system are reformed as

$$\begin{cases}\dot{\hat{x}}(t) = (A + BK)\hat{x}(t) \\ + (L - B(GB)^{-1}GL)(\alpha(t)\varepsilon(t) + (1 - \alpha(t))C\Theta(t)) \\ \dot{\Theta}(t) = A\Theta(t) + Fw(t) \\ - L(\alpha(t)\varepsilon(t) + (1 - \alpha(t))C\Theta(t))\end{cases}. \tag{1.15}$$

1.3 Main Results

In this section, sufficient conditions are established for the closed-loop system (1.15) to be globally asymptotically stable with an L-∞ norm bound. Before presenting the main results, the following useful lemma is introduced.

Definition 1.1 Considering the power system (14), if $w(t) = 0$ and $\varepsilon(t) = 0$, there exists a positive definite continuous first-order partial derivative $V(\hat{x}(t))$ and negative definite $\mathbb{E}\{\dot{V}(\hat{x}(t))\}$. One can conclude that the system is asymptotically stable. Besides, under the zero initial condition of $\hat{x}(t) = 0$, $t \in [-\tau, 0]$, any nonzero $w(t)$, $\varepsilon(t) \in L_2[0, +\infty)$. The disturbance rejection level of H_∞ is given as γ, we have the following condition: $\mathbb{E}\{\|\hat{y}(t)\|_2\} \leq \gamma\mathbb{E}\{\|w(t)\|_2 + \|\varepsilon(t)\|_2\}$.

Lemma 1.1 *For any real vectors u, v and symmetric positive matrix Q with compatible dimensions, the following inequality holds:*

$$u^T v + v^T u \leq u^T Q u + v^T Q^{-1} v.$$

1.3.1 Stability Analysis

Theorem 1.1 *For the given conditions* $1 > \alpha_0 \geq 0$. *System (1.5) is asymptotically stable for the given positive constants* γ *and real symmetric matrices* $Q > 0, W > 0$ *satisfying the following matrix inequality*

$$\begin{bmatrix} \varpi_{11} & \varpi_{12} \\ \varpi_{12}^T & \varpi_{22} \end{bmatrix} < 0, \tag{1.16}$$

where

$$\varpi_{11} = \varpi_a - \varpi_b, \varpi_a = [a_{7*7}], \varpi_b = \Gamma^T\Gamma,$$

$$a_{11} = \mathrm{sym}[X(A + BK)] + Q,$$

$$a_{13} = (1 - \alpha_0)XLC, a_{17} = \alpha_0 XL,$$

$$a_{22} = \delta(j_k h)\phi, a_{25} = -\delta(j_k h)\phi,$$

$$a_{33} = \mathrm{sym}[XA] + W - (1 - \alpha_0)XLC,$$

$$a_{36} = XF, a_{37} = -\alpha_0 XL,$$

$$a_{55} = (\delta(j_k h) - 1)\phi, a_{66} = a_{77} = -\gamma^2 I,$$

$$\Gamma = [(1 - \alpha_0)C \;\; 0^{1*6}],$$

$$\varpi_{12} = \begin{bmatrix} XB & 0 & 0 \\ 0 & 0 & 0 \\ 0 & (1 - \alpha_0)C^T L^T X & 0 \\ 0^{3\times1} & 0^{3\times1} & 0^{3\times1} \\ 0 & 0 & \alpha_0 L^T X \end{bmatrix},$$

$$\varpi_{22} = \begin{bmatrix} -GB & 0 & 0 \\ 0 & -(1 - \alpha_0)X & 0 \\ 0 & 0 & -\alpha_0 X \end{bmatrix}.$$

Proof. Proposing a Lyapunov functional

$$V(t) = V_{\hat{x}}(t) + V_{\Theta}(t), \tag{1.17}$$

where

$$\begin{cases} V_{\hat{x}}(t) = \hat{x}^T(t)X\hat{x}(t) + \int_{t-\tau(t)}^{t} \hat{x}^T(v)Q\hat{x}(v)dv \\ V_{\Theta}(t) = \Theta^T(t)X\Theta(t) + \int_{t-\tau(t)}^{t} \Theta^T(v)W\Theta(v)dv \end{cases}.$$

Calculating the derivative of (1.17), we have

$$\dot{V}(t) = \dot{V}_{\hat{x}}(t) + \dot{V}_{\Theta}(t), \tag{1.18}$$

$$\begin{cases} \dot{V}_{\hat{x}}(t) = 2\hat{x}^T(t)X\dot{\hat{x}}(t) + \hat{x}^T(t)Q\hat{x}(t) \\ \dot{V}_{\Theta}(t) = 2\Theta^T(t)X\dot{\Theta}(t) + \Theta^T(t)W\Theta(t) \end{cases}$$

The expectation of (1.18) is

$$E\{\dot{V}(t)\} = E\{\dot{V}_{\hat{x}}(t) + \dot{V}_{\Theta}(t)\}, \tag{1.19}$$

for

$$\begin{aligned} E\{\dot{V}_{\hat{x}}(t)\} = {} & 2\hat{x}^T(t)X(A+BK)\hat{x}(t) \\ & + 2\alpha_0\hat{x}^T(t)X(L - B(GB)^{-1}GL)\varepsilon(t) \\ & + 2(1-\alpha_0)\hat{x}^T(t)X(L - B(GB)^{-1}GL)C\Theta(t) \\ & + 2\Theta^T(t)XF\omega(t) + \hat{x}^T(t)Q\hat{x}(t) \end{aligned},$$

$$\begin{aligned} E\{\dot{V}_{\Theta}(t)\} = {} & 2\Theta^T(t)XA\Theta(t) - 2\alpha_0\Theta^T(t)XL\varepsilon(t) \\ & - 2(1-\alpha_0)\Theta^T(t)XLC\Theta(t) + \Theta^T(t)W\Theta(t). \\ & + e^T(j_kh)\phi e(j_kh) - e^T(j_kh)\phi e(j_kh) \end{aligned}$$

Noticing that there exist some complex items in (1.19). According to Lemma 1.1, these complex items can be handled like

$$\begin{aligned} & -2\alpha_0\hat{x}^T(t)XB(GB)^{-1}GL\varepsilon(t) \\ & \quad \leq \alpha_0\hat{x}^T(t)XB(GB)^{-1}G\hat{x}(t) + \alpha_0\varepsilon^T(t)L^TXL\varepsilon(t) \end{aligned}.$$

Also, we have

$$\begin{aligned}&-2(1-\alpha_0)\hat{x}^T(t)XB(GB)^{-1}GLC\Theta(t)\\&\quad\leq(1-\alpha_0)\hat{x}^T(t)XB(GB)^{-1}G\hat{x}(t)+(1-\alpha_0)\cdot\\&\quad\times\Theta^T(t)C^TL^TXLC\Theta(t).\end{aligned}$$

Take the event-triggered condition into considering

$$\begin{aligned}&e^T(j_kh)\phi e(j_kh)\\&\quad<\delta(j_kh)(\hat{x}(t-\tau(t))-e(j_kh))^T\phi(\hat{x}(t-\tau(t))-e(j_kh))\end{aligned}.$$

For convenience, we define a matrix as follows

$$\begin{aligned}\xi(t)=\mathrm{col}[&\hat{x}^T(t)\hat{x}^T(t-\tau(t))\Theta^T(t)\Theta^T(t-\tau(t))\\&e^T(j_kh)\omega(t)\varepsilon^T(t)]\end{aligned}.$$

Then

$$\begin{aligned}&\mathbb{E}\{V(t)\}+\mathbb{E}\{\hat{y}^T(t)\hat{y}(t)\}-\gamma^2\mathbb{E}\{\omega^T(t)\omega(t)+\varepsilon^T(t)\varepsilon(t)\}\\&\quad\leq\xi^T(t)(\varpi_{11}-\varpi_{12}\varpi_{22}^{-1}\varpi_{12}^T)\xi(t)\end{aligned}. \tag{1.20}$$

Using the Schur theorem given in [34], (1.20) is concluded as

$$\mathbb{E}\{V(t)\}\leq\gamma^2\mathbb{E}\{\omega^T(t)\omega(t)-\hat{y}^T(t)\hat{y}(t)+\varepsilon^T(t)\varepsilon(t)\}.$$

Integrate the deduction above, we have

$$\begin{aligned}\mathbb{E}\{V(+\infty)\}-\mathbb{E}\{V(0)\}\leq\mathbb{E}\{&\int_0^{+\infty}[-\hat{y}^T(t)\hat{y}(t)\\&+\gamma^2(\omega^T(t)\omega(t)+\varepsilon^T(t)\varepsilon(t))]dt\}\end{aligned}.$$

Under zero initial condition, we can further obtain

$$\mathbb{E}\{\|\hat{y}(t)\|_2\}\leq\gamma\mathbb{E}\{\|\omega(t)\|_2\}+\mathbb{E}\{\|\varepsilon(t)\|_2\}. \tag{1.21}$$

When $\omega(t)=0$ and $\varepsilon(t)=0$, the inequality is concluded as

$$\mathbb{E}\{\dot{V}(t)\}\leq-\mathbb{E}\{\hat{y}^T(t)\hat{y}(t)\}<0. \tag{1.22}$$

Then, there exists a positive scalar $\epsilon>0$ that makes the following inequality holds

$$\mathbb{E}\{\dot{V}(t)\}\leq-\epsilon\mathbb{E}\{\|\hat{x}(t)\|^2\}. \tag{1.23}$$

Based on the proposed control scheme, the multi-area power system to be robustly stable with an optimal attenuation level γ. It completes the proof.

Corollary 1.1 *System (1.5) is asymptotically stable for the given conditions $\alpha_0 \geq 0$, if there exist matrixes $Q > 0$ and $W > 0$, appropriate known positive number $\gamma > 0$, real symmetric matrixes $\chi > 0$, and an arbitrary matrix Y satisfying the following LMI*

$$\begin{bmatrix} \tilde{\varpi}_{11} & \tilde{\varpi}_{12} & \tilde{\varpi}_{13} \\ * & \tilde{\varpi}_{22} & 0^{1*3} \\ * & * & -I \end{bmatrix} < 0, \tag{1.24}$$

where

$$\tilde{\varpi}_{11} = [\tilde{a}_{7*7}]\,, \tilde{a}_{11} = \mathrm{sym}[A\chi + BY] + \chi Q \chi,$$

$$\tilde{a}_{13} = (1-\alpha_0)LC\chi, \tilde{a}_{17} = \alpha_0 L,$$

$$\tilde{a}_{22} = \delta(j_k h)\phi, \tilde{a}_{25} = -\delta(j_k h)\phi,$$

$$\tilde{a}_{33} = \mathrm{sym}[A\chi] + \chi W \chi - (1-\alpha_0)LC\chi,$$

$$\tilde{a}_{36} = F, \tilde{a}_{37} = -\alpha_0 L,$$

$$\tilde{a}_{55} = (\delta(j_k h) - 1)\phi, \tilde{a}_{66} = \tilde{a}_{77} = -\gamma^2 I,$$

$$\tilde{\varpi}_{13} = [(1-\alpha_0)C\chi \;\; 0^{1*6}]^T,$$

$$\tilde{\varpi}_{12} = \begin{bmatrix} B & 0 & 0 \\ 0 & 0 & 0 \\ 0 & (1-\alpha_0)\chi^T C^T N^T & 0 \\ 0^{3\times1} & 0^{3\times1} & 0^{3\times1} \\ 0 & 0 & \alpha_0 L^T \end{bmatrix},$$

$$\tilde{\varpi}_{22} = \begin{bmatrix} -GB & 0 & 0 \\ 0 & -(1-\alpha_0)\chi & 0 \\ 0 & 0 & -\alpha_0\chi \end{bmatrix}.$$

Proof. Define $\chi = X^{-1}$ and $Y = K\chi$, pre- and post-multiplying both sides of inequality (1.16) with diag$\{\chi, I, \chi, I, I, I, I, I, \chi, \chi\}$.

We can notice that the matrix in Theorem 1.2 cannot be solved directly. The reason is for the nonlinear terms $LC\chi$, $\chi W\chi$ and $\chi Q\chi$. To deal with the nonlinear term $LC\chi$ in Theorem 1.2, we have added the following theorem. So that the nonlinear problem is solvable. Besides, $\chi W\chi$ and $\chi Q\chi$ are defined as $\chi W\chi = \tilde{W}$ and $\chi Q\chi = \tilde{Q}$, respectively.

Theorem 1.2 *Based on Corollary 1.1, for the given full-rank matrix M and any proper matrix N with appropriate dimensions, such that (1.24) holds, and the following LMI*

$$\begin{bmatrix} \tilde{\varpi}'_{11} & \tilde{\varpi}'_{12} & \tilde{\varpi}_{13} \\ * & \tilde{\varpi}_{22} & 0^{1*3} \\ * & * & -I \end{bmatrix} < 0, \tag{1.25}$$

$$\begin{bmatrix} \xi I & C^T M^T - X^T C^T \\ * & -I \end{bmatrix} < 0, \tag{1.26}$$

where ξ is approaching to 0, $\tilde{\varpi}'_{11}$ and $\tilde{\varpi}'_{12}$ are obtained from $\tilde{\varpi}_{11}$ and $\tilde{\varpi}_{12}$ by replacing $LC\chi$ with NC and replacing $\chi W\chi$, $\chi Q\chi$ with $\tilde{W}$, $\tilde{Q}$ respectively, the system is asymptotically stable with observer gains $L = NM^{-1}$. It completes the proof.

Remark 1.1: Based on the proposed sliding mode LFC scheme, Theorem 1.2 could guarantee the attacked multi-area power system to be robustly stable with an optimal attenuation level γ. In Theorem 1.2, the nonlinear coupling terms have been replaced by processable terms.

1.3.2 Control Law Design

For SMC theory, a proper sliding control law is of great importance. The trajectory of the power system shall be reachable to the sliding surface in a limited time under the supplied controller. For the controlled multi-area power system (1.5), the corresponding reachability condition for the i-th area can be described by the following theorem.

Theorem 1.3 *For the considered sliding mode surface (1.9), a proper control law is given as*

$$\begin{aligned} u(t) = {} & K\hat{x}(t) - (1-\alpha(t))(GB)^{-1}GLC\Theta(t) \\ & - h_i(GB)^{-1}\sigma_i(t) - h_i(GB)^{-1}\|GF\|\mathrm{sgn}(\sigma_i(t)) \end{aligned}, \tag{1.27}$$

where h_i is a positive constant, and $\mathrm{sgn}(\sigma_i(t))$ *is the switching function that*

$$\mathrm{sgn}(\sigma_i(t)) = \begin{cases} -1, & \text{if } \sigma_i(t) < 0 \\ 0, & \text{if } \sigma_i(t) = 0. \\ 1, & \text{if } \sigma_i(t) > 0 \end{cases}$$

Proof. The Lyapunov function is constructed as

$$V_L = \frac{1}{2}\sigma_i^T(t)\sigma_i(t). \tag{1.28}$$

From (1.12), (1.27), and (1.28), the derivative of $V_L(t)$ is

$$\begin{aligned} \dot{V}_L = {} & \frac{1}{2}\dot{\sigma}_i^T(t)\sigma_i(t) + \frac{1}{2}\sigma_i^T(t)\dot{\sigma}_i(t) \\ = {} & \sigma_i^T(t)\dot{\sigma}_i(t) \\ = {} & \sigma_i(t)[-GBK\hat{x} + GBu(t) + (1-\alpha(t))GLC\Theta(t)] \\ = {} & \sigma_i(t)[-GBK\hat{x} + (1-\alpha(t))GLC\Theta(t) \\ & + GB(K\hat{x}(t) - (1-\alpha(t))(GB)^{-1}GLC\Theta(t) \\ & - h_i(GB)^{-1}\sigma_i(t) - h_i(GB)^{-1}\|GF\|\mathrm{sgn}(\sigma_i(t)))] \\ = {} & -h_i\|\sigma_i(t)\|^2 - h_i\sigma_i(t)\|GF\|\mathrm{sgn}(\sigma_i(t)) \\ < {} & -h_i\|\sigma_i(t)\|^2 - h_i\|\sigma_i(t)\|\|GF\| < 0 \end{aligned}.$$

Therefore, one can conclude that the system can be kept stable by the designed control law (1.27).

Remark 1.2: The variable structure control has the advantages of fast response and being insensitive to parameter changes and disturbances. The way of SMC can be designed and independent of plant parameters and disturbances. This method can be simply implemented in physical. The main disadvantage, however, is that the imperfections of all kinds of components of the actual system may contribute to causing the control switching delay. Specifically, when the state trajectory reaches the sliding surface, it is difficult to slide strictly along the sliding surface toward the equilibrium point. Instead, it may pass back and forth on both sides of the sliding surface, resulting in chattering. The error of the operation in MATLAB. Besides, the use of SMC will certainly cause some buffeting phenomena.

1.4 Numerical Examples

In this section, numerical examples are provided to demonstrate the effectiveness of the proposed design scheme. Take a three-area interconnected power system as an example. The simulation results verify the effectiveness and correctness of the proposed SMC scheme. By analyzing the simulation diagram, one can conclude that the system can reach a stable state under the designed SMC.

Parameter values of the three-area interconnected power system are presented in Table 1.2. We consider a three-area interconnected power system. By using the MATLAB LMI control toolbox, the stability condition could be verified effectively.

The controller gain and observer gain can be calculated as

$$K = \begin{bmatrix} -223.783 & -5.012 & -3.280 & 91.864 & 1.795 \\ -157.956 & -2.073 & -2.597 & 67.533 & 1.631 \\ -160.963 & -2.360 & -2.448 & 69.519 & 1.510 \end{bmatrix},$$

$$L = \begin{bmatrix} 0.272 & 1.219 & -0.280 & 0.075 & -0.116 \\ 0.108 & -0.04 & -0.224 & 0.019 & -0.295 \\ 0.207 & -0.017 & -0.292 & 0.063 & -0.135 \end{bmatrix}^T.$$

Under the control scheme, the frequency derivative of the power system is shown in Figure 1.2. It can be seen that with the designed control scheme, the frequency derivative value of the deception-attacked power system gradually tends to a stable state. This demonstrates that the proposed controller can effectively

Table 1.2 Parameters of three-area interconnected power system.

D_1, D_2, D_3	1, 1.5, 1.8
$T_{ch1}, T_{ch2}, T_{ch3}$	0.3, 0.17, 0.2
T_{g1}, T_{g2}, T_{g3}	0.37, 0.4, 0.35
R_1, R_2, R_3	0.05, 0.05, 0.05
beta1, beta2, beta3	21, 21.5, 21.8
$P_{d1}, P_{d2}, P_d 3$	0.1, 0.1, 0.1
$\gamma_1,\gamma_2,\gamma_3,$	2, 2, 2

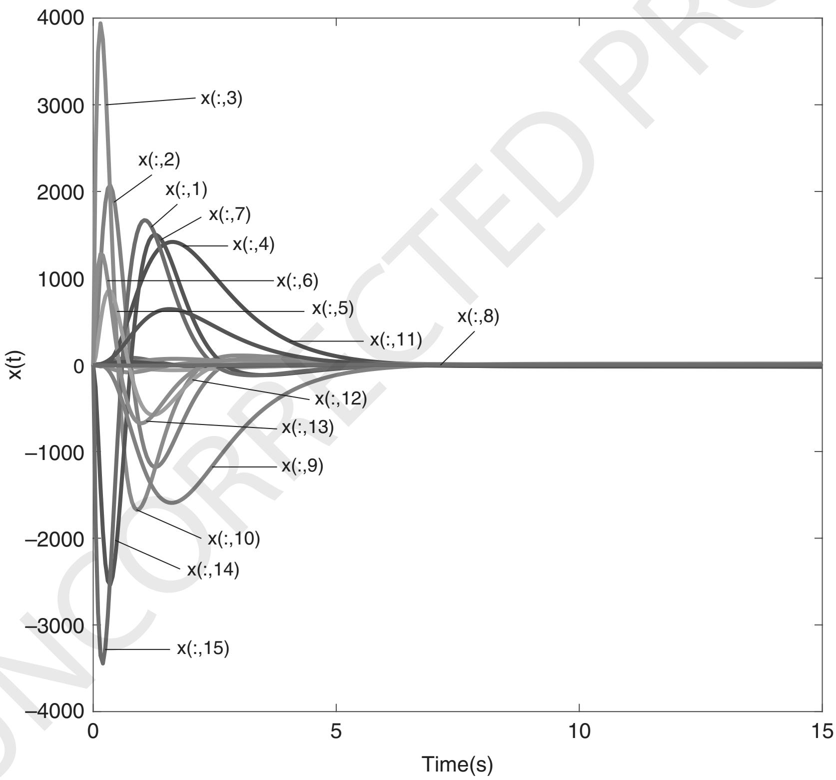

Figure 1.2 Frequency deviation of power system.

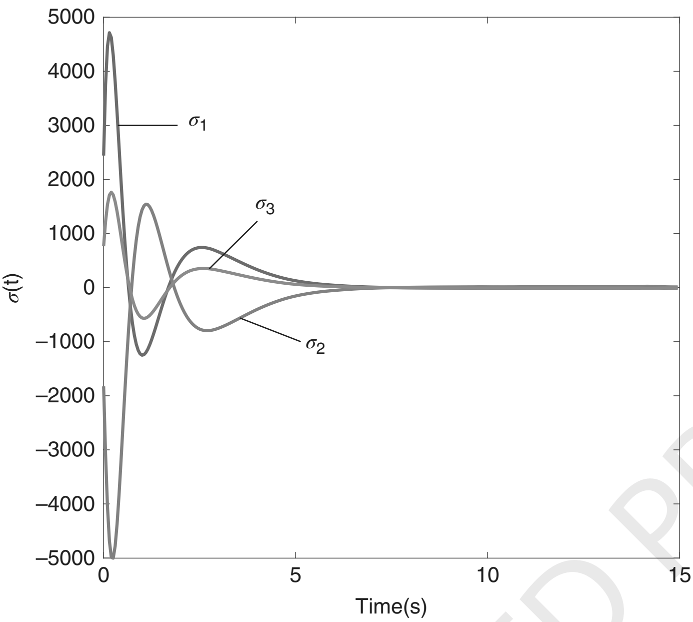

Figure 1.3 Designed sliding mode surface (SMC).

reduce the frequency deviation of the system, improving the robustness of the attacked power system. This is, the power system can be stable under SMC, although it was attacked.

The designed sliding surface trajectory is shown in Figure 1.3. It can be seen from the figure that the sliding surface can reach a stable state in a certain period and keep running. One can prove that the sliding mode that we designed can work normally and satisfies our purpose.

It can be seen from Figure 1.4 that the power system under deception attack with equivalent control can operate to a stable state over time. The test condition is listed in Table 1.2 and the controller gain is calculated as K. This means the power system can work in a stable state under the provided control method.

To ensure that the system can reach the sliding surface in a limited time, the state trajectory of the SMC law is shown in Figure 1.5. According to the curve, the simulation results can easily show the effectiveness of the proposed sliding mode LFC scheme.

We test on the case where something is random, the event-trigger frequency and probability are equally random. Figure 1.6 shows the event interval during the deception attack. The disorder event is shown in Figure 1.6, conforming to our requirements for random attacks.

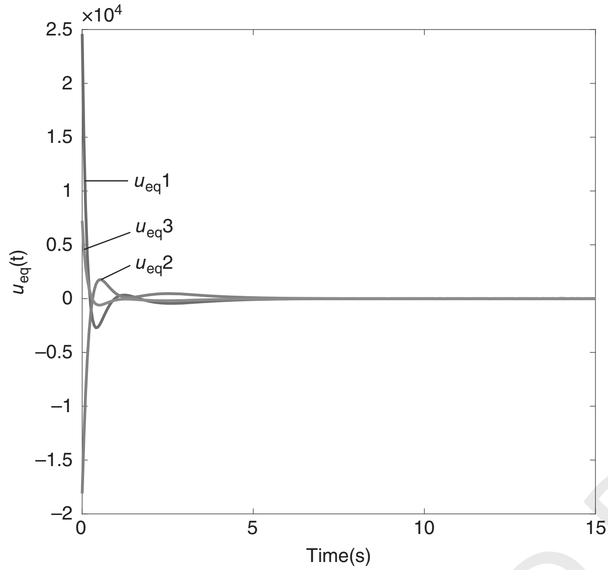

Figure 1.4 Equivalent control of sliding mode controlled power system.

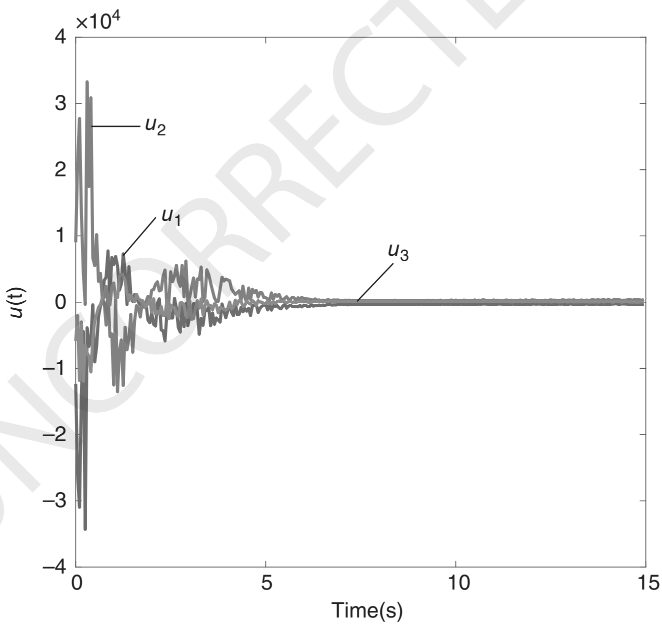

Figure 1.5 State of SMC law.

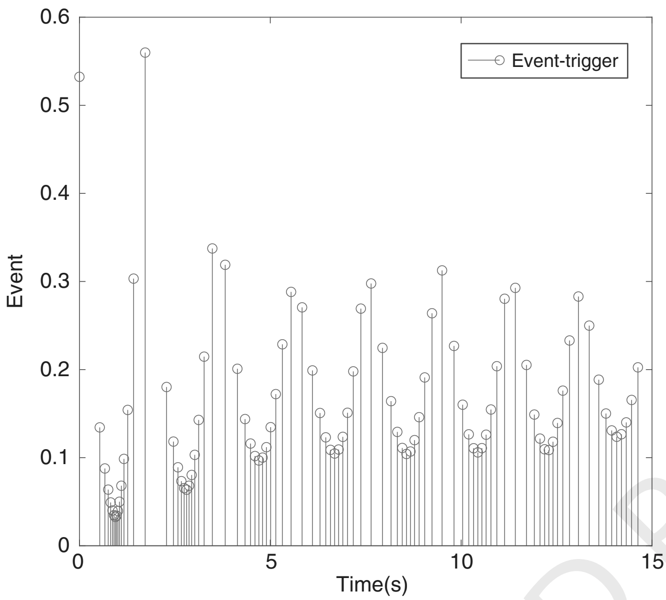

Figure 1.6 Event interval during deception attack interval.

1.5 Conclusion

An observer-based event-triggered transmission scheme was proposed for multi-area power systems. To be specific, an observer has been provided to gain disturbed transmission information. An event-trigger scheme is added to determine whether the information should be transmitted. On the basis of the above analysis, a sliding mode controller has been constructed to keep the stability of the multi-area power system which is injured by some attack. This chapter has only considered a kind of deception attack. In fact, it is possible that several attacks influence the system at the same time. The modeling of attack is also a problem worthy of consideration. In addition, with more and more renewable energy access to the power grid, its inherent randomness and uncertainty should be paid attention to.

References

1 R. W. Kenyon, M. Bossart, M. Markovi, et al. Stability and control of power systems with high penetrations of inverter-based resources: An accessible review of current knowledge and open questions. *Solar Energy*, 210:149–168, 2020.

2 H. Ahsan and M. D. Mufti. Comprehensive power system stability improvement with rocof controlled smes. *Electric Power Components and Systems*, 48:162–173, 2020.

3 A. C. Xue, J. H. Zhang, L. J. Zhang, et al. Transient frequency stability emergency control for the power system interconnected with offshore wind power through VSC-HVDC. *IEEE Access*, 8:53133–53140, 2020.

4 X. Lv, Y. Sun, Y. Wang, and V. Dinavahi. Adaptive event-triggered load frequency control of multi-area power systems under networked environment via sliding mode control. *IEEE Access*, 8:86585–86594, 2020.

5 Y. M. Alsmadi, A. Alqahtani, R. Giral, et al. Sliding mode control of photovoltaic based power generation systems for microgrid applications. *International Journal of Control*, 94:1704–1715, 2021.

6 M. Y. Silaa, M. Derbeli, O. Barambones, and A. Cheknane. Design and implementation of high order sliding mode control for PEMFC power system. *Energies*, 13:4317–4332, 2020.

7 A. T. Tran, B. Le Ngoc Minh, P. T. Tran, et al. Adaptive integral second-order sliding mode control design for load frequency control of large-scale power system with communication delays. *Complexity*, 2021:5564184, 2021.

8 R. Nie, S. He, F. Liu, and X. L. Luan. Sliding mode controller design for conic-type nonlinear semi-Markovian jumping systems of time-delayed Chua's circuit. *IEEE Transactions on Systems*, 51:2467–2475, 2021.

9 G. Q. Zhu, L. Nie, Z. Lv, et al. Adaptive fuzzy dynamic surface sliding mode control of large-scale power systems with prescribe output tracking performance. *ISA Transactions*, 99:305–321, 2020.

10 X. Lv, Y. Sun, W. Hu, and V. Dinavahi. Robust load frequency control for networked power system with renewable energy via fractional-order global sliding mode control. *IET Renewable Power Generation*, 15:1046–1057, 2021.

11 A. T. Tran, B. Le Ngoc Minh, V. V. Huynh, et al. Load frequency regulator in interconnected power system using second-order sliding mode control combined with state estimator. *Energy*, 14:863–880, 2021.

12 M. Elsisi, N. Bazmohammadi, J. M. Guerrero, and M. A. Ebrahim. Energy management of controllable loads in multi-area power systems with wind power penetration based on new supervisor fuzzy nonlinear sliding mode control. *Energy*, 221:119867–119881, 2021.

13 S. P. He, W. Z. Lyu, and F. Liu. Robust sliding mode controller design of a class of time-delayed discrete conic-type nonlinear systems. *IEEE Transactions on Systems, Man, and Cybernetics: Systems*, 51:885–892, 2021.

14 W. H. Qi, G. D. Zong, and W. X. Zheng. Adaptive event-triggered smc for stochastic switching systems with semi-Markov process and application to boost converter circuit model. *IEEE Transactions on Circuits and Systems I: Regular Papers*, 68:786–796, 2020.

15 S. H. Huang and J. Wang. Fixed-time fractional-order sliding mode control for nonlinear power systems. *Journal of Vibration and Control*, 26:1425–1434, 2020.

16 V. V. Huynh, B. Le Ngoc Minh, E. N. Amaefule, et al. Highly robust observer sliding mode based frequency control for multi area power systems with renewable power plants. *Electronics*, 10:274–294, 2021.

17 N. K. Singh and V. Mahajan. Analysis and evaluation of cyber-attack impact on critical power system infrastructure. *Smart Science*, 9:1–13, 2021.

18 X. C. ShangGuan, Y. He, C. K. Zhang, et al. Switching system-based load frequency control for multi-area power system resilient to denial-of-service attacks. *Control Engineering Practice*, 107:104678–104689, 2021.

19 L. Zhao and W. Li. Co-design of dual security control and communication for nonlinear CPS under DoS attack. *IEEE Access*, 8:19271–19285, 2020.

20 B. Hu, H. Wang, Y. Zhao, et al. A brief overview of optimal robust control strategies for a benchmark power system with different cyber-physical attacks. *Complexity*, 2021(1):6646799, 2021

21 W. H. Qi, Y. K. Hou, G. D. Zong, and C. Ki Ahn. Finite-time event-triggered control for semi-Markovian switching cyber-physical systems with FDI attacks and applications. *IEEE Transactions on Circuits and Systems I: Regular Papers*, 68:2665–2674, 2021.

22 Z. H. Pang and G. P. Liu. Design and implementation of secure networked predictive control systems under deception attacks. *IEEE Transactions on Control Systems Technology*, 20:1334–1342, 2011.

23 M. R. Habibi, H. R. Baghaee, F. Blaabjerg, and T. Dragievi. False data injection cyber-attacks mitigation in parallel DC/DC converters based on artificial neural networks. *IEEE Transactions on Circuits and Systems II: Express Briefs*, 68:717–721, 2020.

24 D. J. Du, R. Chen, X. Li, et al. Malicious data deception attacks against power systems: A new case and its detection method. *Transactions of the Institute of Measurement and Control*, 41:1590–1599, 2019.

25 Y. Li, P. Zhang, B. Wang, and L. Zhang. Active synchronous detection of deception attacks in microgrid control systems. *IEEE Transactions on Smart Grid*, 8:373–375, 2016.

26 R. C. Borges Hink, J. M. Beaver, M. A. Buckner, et al. Machine learning for power system disturbance and cyber-attack discrimination. *7th International Symposium on Resilient Control Systems*, pages 1–8, 2014.

27 D. Zhao, Z. D. Wang, G. L. Wei, et al. A dynamic event-triggered approach to observer-based PID security control subject to deception attacks. *Automatica*, 120:109128–109141, 2020.

28 J. Shi. Cooperative control for nonlinear multi-agent systems based on event-triggered scheme. *IEEE Transactions on Circuits and Systems II: Express Briefs*, 68:1977–1981, 2020.

29 E. Tian and C. Peng. Memory-based event-triggering h_∞ load frequency control for power systems under deception attacks. *IEEE Transactions on Cybernetics*, 50:4610–4618, 2020.

30 D. J. Wang, F. Chen, B. Meng, et al. Event-based secure h_∞ load frequency control for delayed power systems subject to deception attacks. *Applied Mathematics and Computation*, 394:125788–125801, 2021.

31 W. Shen, S. Liu, and M. Liu. Adaptive sliding mode control of hydraulic systems with the event-trigger and finite-time disturbance observer. *Information Sciences*, 569:55–69, 2021.

32 Md. M. Hossain and C. Peng. Observer-based event-triggering h_∞ lfc for multi-area power systems under dos attacks. *Information Sciences*, 543:437–453, 2021.

33 D. Yue, E. Tian, and Q. L. Han. A delay system method for designing event-triggered controllers of networked control systems. *IEEE Transactions on Automatic Control*, 58:475–481, 2013.

34 S. Boyd, L. El Ghaoui, E. Feron, et al. *Linear Matrix Inequalities in System and Control Theory*. Philadelphia: SIAM, 1994.